Power-hardware-in-the-loop approach for emulating an offshore wind farm connected with a VSC-based HVDC

Torres Olguin, R.; Endegnanew, A.; D'Arco, S. & Morel, A.

Power-Hardware-in-the-Loop approach for emulating an offshore wind farm connected with an VSC-based HVDC

Raymundo E. Torres-Olguin, Atsede G. Endegnanew, Salvatore D'Arco
SINTEF Energy Research
Trondheim, Norway
Adrien Morel
Ecole Centrale de Lyon
Lyon, France
Contact email: raymundo.torres-olguin@sintef.no

***Abstract*—The real-world interaction of an offshore wind farm with a voltage source converter (VSC)-based HVDC is complex due issues such as noise, randomness of event timings, and hardware design issues that are not well explored. Numerical simulations are widely accepted and cost effective tool to test a wide variety of different cases, however, the fidelity of the results is difficult to assess. Higher fidelity can be obtained with scale-down experiments, however, this solution has a limited test coverage. The power-hardware-in-the-loop (PHIL) approach offers a good trade-off between test fidelity and test coverage. The hardware part allows a high fidelity of the results whereas, the software simulation part allows an extensive study of different cases at a reasonable cost. This paper presents a PHIL implementation of an offshore wind farm connected with a VSC-based HVDC. The offshore wind farm is emulated in a real time simulation environment, and a grid emulator is used as power interface between the emulated system and the hardware system, i.e. VSC-based HVDC substation. The interaction of real time models and hardware is demonstrated with experiment results.**

I. Introduction

In the near future, offshore wind energy is predicted to be the predominant renewable sources of energy that can help to accommodate much of the ever increasing energy demand. However, high penetration of offshore wind energy represents a unprecedented challenge of the grid integration due the intermittent and nondispatchable nature of the wind resource [1]. Moreover, the interconnection of resource located far away of the connection point suggests high voltage direct current (HVDC) solutions [2]. The dominant technology in HVDC is based on current source converters (CSC) or line commutated converter (LCC) [3]. However, the use LCC technology is discarded due the filtering requirement that make a large footprint that is non-viable in offshore applications. Therefore, voltage source (VSC)-based HVDC technology is an attractive solution because of the ability to operate active and reactive power flows independently, start up capability and relatively small footprint in offshore installations [4].

Numerical simulations have been widely accepted for interconnection studies of renewable sources and HVDC. The accuracy of the numerical simulations are limited by the mathematical models of each component. The complexity of the models depend on the computation resources and it reflects on the simulation running time. Scaled experiments are an irreplaceable step before the real application. However, scaled experiments are expensive, and less flexible if some reconfiguration is needed. Hardware-in-the-loop (HIL) is a relatively new trend of combining simulation models that are synchronized with a real-time clock, i.e. real-time simulation models, and key hardware elements of the system. This approach provides flexibility in recreating wide range of operating conditions, i.e. improve the test coverage while the hardware can give a very accurate results. Moreover, power amplifiers can be installed in the HIL approach, which is called power-hardware-in-the-loop (PHIL), to interface with power equipments such as converters, transformers or electrical machines. The power amplifier can provide or absorb power, since it has a bidirectional structure, the hardware under test can be tested with actual power exchange. There are several examples of HIL in different fields such as automotive systems [5] [6], robotics [7], and power system [8]. In power electronics, PHIL has been used to study energy storage [9], electric drives [10], microgrids [11], etc. There are several examples of HIL and PHIL related with the integration of wind farms. In [13], a HIL implementation of a real variable speed wind turbine using squirrel-cage induction generator interacting with a emulated turbine and electrical network is presented. A HIL-based simulator for a variable-speed wind turbines is developed in [14] where simulated plant interacting with the real controller. In [12], a PHIL implementation of variable-speed wind turbines connected with a microgrid testbed is presented. This paper addresses the PHIL approach for emulating an offshore wind farm connected with an VSC-HVDC. In the simulation environment, an aggregate model of a variable-speed wind farm is considered. The equivalent wind turbine contains a fully rated converter connected to a gearless permanent magnet synchronous machine. The HVDC substation is included in the hardware environment, i.e. a two-level converter that interact with a grid emulator, which received

reference from the simulation environment. The structure of this paper is as follows: Section II develops the modeling of PMSG -based wind turbine. Section III describes the PHIL setup. Section IV presents experimental results. Section V gives some concluding remarks.

II. Modeling of the wind farm

Variable-speed wind turbines using fully rated converters (FRC) are an attractive solution for offshore. This configuration has a number of advantages which include: (i) wide speed range of operation (ii) independent control of active and reactive power to the grid (iii) reduced mechanical stress. In this paper, the configuration FRC has been selected to investigate the interaction between the VSC-based HVDC system and the offshore wind farm. It is also expected that most of the turbines will be of this type in future developments.

Currently, wind farm manufactures have a number of different options for FRC-based wind turbines. Some examples include geared synchronous machine based (e.g. Vestas V112, Gamesa G128, Kenersys K82), gearless synchronous machine-based (e.g. Lagerwey L82) and geared asynchronous machine-based (ABB) wind turbines. In this paper the configuration shown in Figure 2, which is based on a gearless synchronous generator connected with a back-to-back converter is considered.

The control schemes discussed in this paper are applicable to any synchronous generator with IGBT converters regardless of either geared or gearless drive train. The rotor model and the control strategy of the PMSG-based wind turbine are presented below.

A. Rotor model

The power P_w that can be extracted by the turbine as mechanical power, in this case a three-bladed horizontal-axis wind turbine, is given by

$$P_w = \frac{1}{2}\rho A C_p(\beta, \lambda)\, v_w^3 \tag{1}$$

where ρ is the air density, A is the swept area of the blades, v_w is the wind speed, and C_p is the power coefficient function. C_p is a function of the of the pitch angle β and the tip speed ratio λ which defines the performance of a wind turbine and is defined as the relation between rotor speed ω and wind speed v_w, as shown below:

$$\lambda = \frac{\omega_r R}{v_w}$$

where R is the turbine radius. There are several methods to determine C_p such as blade element theory, lookup tables, and analytical approximations [15]. This paper uses the following numerical approximation for given values of β and λ

$$C_p(\beta, \lambda) = 0.51\left(\frac{116}{\lambda_i - 0.4\beta - 5}\right)e^{\frac{-21}{\lambda_i}} + 0.0068\lambda$$

where

$$\lambda_i = \left(\frac{1}{\lambda + 0.08\beta} - \frac{0.035}{\beta^3 + 1}\right)^{-1}$$

As can be seen from (1), the maximum power is directly proportional to C_p. Optimum C_p for a given β is achieved by changing λ. This is the reason for using variable-speed turbines; when the wind changes, a variable-speed turbine is able to adjust the speed to achieve optimum power coefficient and hence maximum power from the wind can be extracted. The drive train is modeled using a one-mass model. This means that the rotor uses a lumped mass model and the dynamics of the shaft is neglected. The mathematical expression of the one-mass model is given by:

$$2H\frac{d}{dt}\omega_r = T_m - T_e \tag{2}$$

where H is the inertia constant, ω is the rotor speed, and T_m and T_e are the mechanical and electric torques. The accuracy of the one-mass model is sufficient when considering the decoupling between the grid and the turbine through the power converter.

B. Control of PMSG-based wind turbine

The controller design of the turbine can be divided into two parts: the generator side (GSC), and the AC grid side controller (ACGC). The GSC controls the rotor speed to achieve the maximum power at low wind conditions and the ACGS regulates the DC-link voltage for the proper operation of the back-to-back converter. More details about each part of the turbine controller are given below.

1) Generator side controller: The objective of the GSC is to extract the maximum power in the variable speed region described above. The GSC directly controls the power using the steady-state characteristic of the wind turbine shown in Figure 1. This steady-state characteristic shows the output mechanical power versus the turbine rotor speed ω with no pitch control action.

As can be seen in Figure 1, for a given rotor speed, and for each wind speed, there is a maximum power point (MPPT). The optimum power line is formed by the points of maximum power. The task of the GSC controller is to track the MPPT

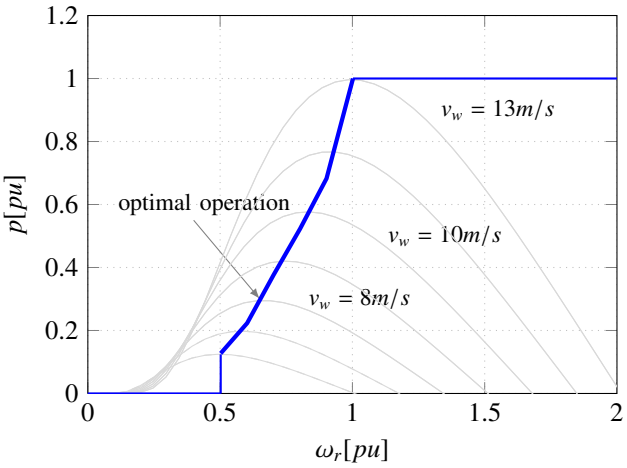

Figure 1: Rotor-speed wind characteristic

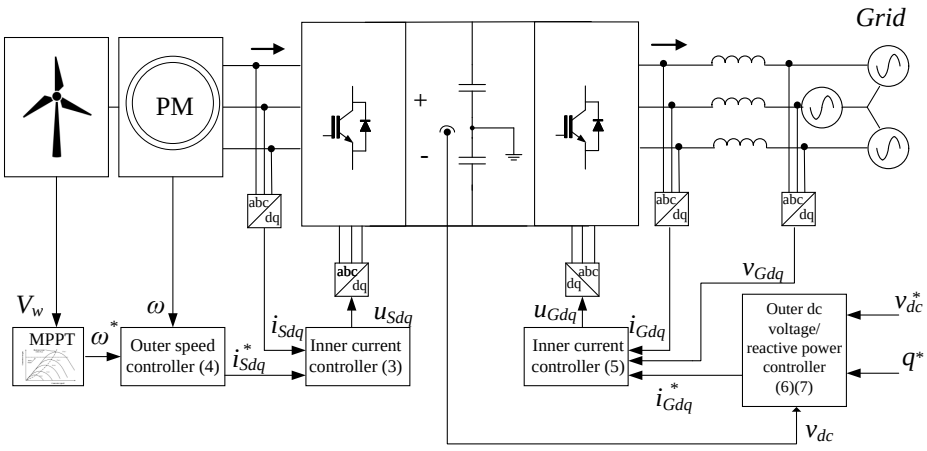

Figure 2: Block diagram of the GSC and ACGS controllers of the wind turbine

for any particular wind condition. The idea is to operate over the optimal power line such that the maximum power can be continuously extracted from the wind.

To facilitate the controller design, the d-axis has been aligned with the rotor flux Ψ, hence q-axis is 90° ahead of the d-axis. The decoupling assumption is used, so Vector control allows the torque and the flux magnitude of the machine to be controlled independently. The objective of the inner loop is to control the regulation of $\boldsymbol{i}_{Sdq}$ towards its reference, $\boldsymbol{i}^*_{Sdq} = \left[i^*_{Sd}\ i^*_{Sq}\right]^\top$. The inner loop regulates $\boldsymbol{i}_{Sdq}$. The cross-coupling terms are eliminated, and a proportional term k_{p1} allows the regulation of $\boldsymbol{i}_{Sdq}$ towards its reference. Here, $\boldsymbol{u}_{Sdq}$ takes the following form:

$$\boldsymbol{u}_{Sdq} = -L_S\omega_r\mathbf{J}\boldsymbol{i}_{Sdq} + \omega_r\left[0,\Psi\right]^\top + k_{p1}\tilde{\boldsymbol{i}}_{Sdq} \tag{3}$$

Since the q-axis is 90° ahead of the d-axis in the direction of rotor rotation.The outer loop can regulates the speed using a simple PI acting over that produces the reference i^*_{Sq}. The i^*_{Sq} is written as

$$i^*_{Sq} = \left(k_{p2} + \frac{k_{i2}}{s}\right)\tilde{\omega} \tag{4}$$

where $\tilde{\omega} \triangleq \omega^* - \omega$ and ω^* is the reference turbine speed. k_{p2} and k_{i2} are the proportional and integral gains of the PI controller. i^*_{Sd} which is kept at zero to minimize resistive losses. Notice that ω^* can be obtained using the optimal line illustrated above in Figure 1.

2) AC grid side controller: In this approach, the d-axis is aligned with the offshore ac voltage. Under these conditions active power and reactive power are decoupled. As with the case of GSC, the control design is divided into two loops: inner and outer. The inner loop has the same objective of regulating the current $\boldsymbol{i}_{Gdq}$ towards its reference. The following controller $\boldsymbol{u}_{Gdq}$ is proposed:

$$\boldsymbol{u}_{Gdq} = L_G\omega\mathbf{J}\boldsymbol{i}_{Gdq} + \boldsymbol{v}_{Gdq} + \left(k_{p3} + \frac{k_{i3}}{s}\right)\tilde{\boldsymbol{i}}_{Gdq} \tag{5}$$

where k_{p3} and k_{i3} are the proportional and integral gains of the PI controller.

The outer loop regulates the DC voltage v_{dc} in the DC link voltage of the back-to-back converter. The v_{dc} can be controlled using the following control:

$$i^*_{Gd} = -\left(k_{p4} + \frac{k_{i4}}{s}\right)\tilde{v}_{dc} \tag{6}$$

where $\tilde{v}_{dc} \triangleq v^*_{dc} - v_{dc}$; v^*_{dc} is the reference of the DC voltage. k_{p4} and k_{i4} represent the parameters of the PI controller. The outer loop can also regulates the reactive power.

III. Power Hardware-in-the-Loop Implementation

Figure 3 shows the PHIL platform for emulating the wind farm with a VSC-based HVDC. In the simulated wind farm, it was considered that wind speed and voltage measured in a two-level VSC, v_{abc}, as inputs as shown in Figure 3. The output of the model is the reference currents, $i_{abc}*$ for the grid emulator. In the hardware section, a two-level VSC generates a three-phase ac voltage with a fixed frequency i.e. operating in island mode. A transformer is connected to the three-phase ac current output of the grid emulator. A real time simulation platform is used to control and monitor the the following:

- Dc voltage of the grid emulator
- Island mode control of the hardware converter
- Simulation of a wind turbine using the Simulink model to generate a current reference of the grid emulator

A. Wind farm model

The wind farm, which uses an aggregate approach, is designed assuming a 2 MW generation system connected to a 690 V and 50 Hz grid and operating at 1500 V dc voltage. In this paper a configuration shown in Figure 1, which is based on a back-to-back IGBT converters and a permanent magnet synchronous generator with gearless drive train. . The main parameters are shown in the appendix. The control schemes discussed previously are applicable to any synchronous generator regardless the drive train, i.e. either geared or gearless

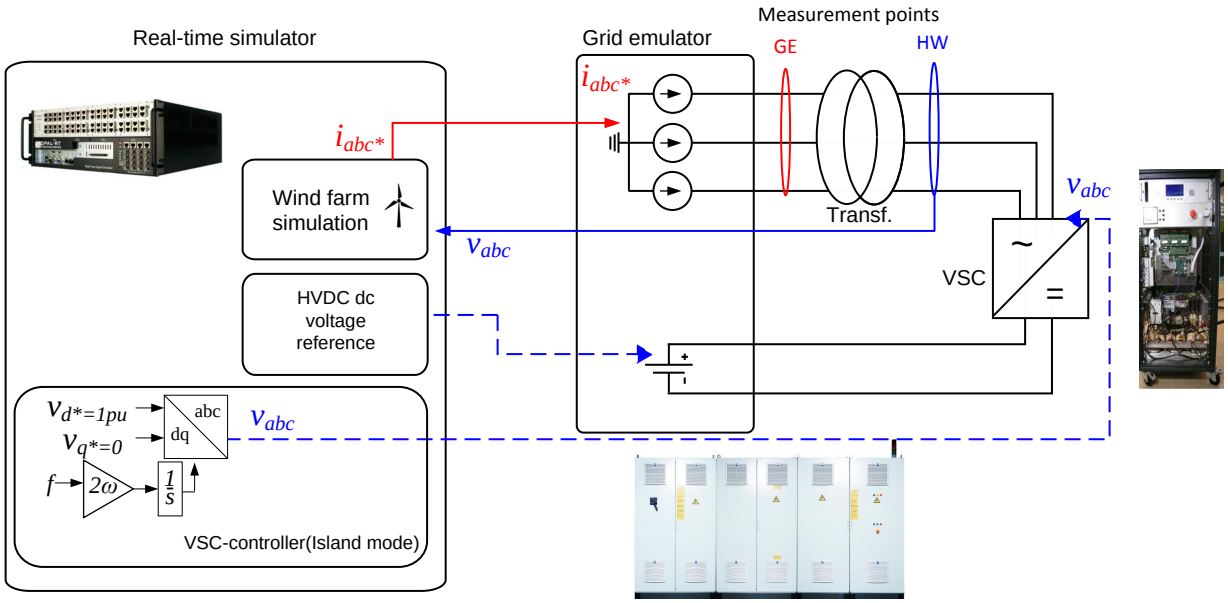

Figure 3: PHIL implementation

drive train. Wind turbines have been emulated by scaling to 18 kW.

B. Real time simulator

For a PHIL setup, the model on the software side has to be run in real time. To that extent, the Simulink model is translated into C code with a software called RT-Lab. This translated model is then run on a simulation platform: OP5600 from Opal RT. This platform is designed to run real time electro-magnetic transient simulations thanks to its four processor cores running at 3.47 GHz. For this implementation, all of the following is controlled in the real time simulator:

- Wind turbine model and wind interface
- Hardware converter control and interface
- Grid emulator control and interface

In this work, all the different subsystems described in Figure 3 are run with a 100 μs time step.

C. Grid Emulator

The grid emulator is an Egston CSU 200: Compiso System Unit 200kVA with six outputs. Three outputs are used as a three-phase ac current sources with a magnitude limited to 14 A rms. Two outputs are used to generate the dc voltage of the HVDC link at 700 V. The grid emulator is controlled by the Simulink interface connected to the OP5600 platform.

D. VSC-based HVDC

The voltage source converters are rated to 60 kVA. The whole device is composed by: converter, LCL smoothing filter, switchgear, and the control system. The converters use two-level configuration based on insulated gate bipolar transistors (IGBTs) which is switching at 10 kHz. The grid connection is through a LCL filter with the following parameters: converter-side filter inductor 50 mH, capacitor 20 μF and grid side filter inductor 200 mH. In order to isolate the converter from the power source i.e. grid emulator, the converter is connected to a delta-wye 1:1 transformer connected to the grid emulator. The control of the hardware converter is included in the Simulink model and the interface allows to display the ac voltage and current, and the dc voltage. It also allows the user to choose the frequency and amplitude of the ac output as is needed. The controller is shown in Figure 3, which is an island mode where amplitude and frequency is fixed.

E. Scaling

As the hardware converters available in the laboratory are scaled down version of converters for offshore wind power integration, their rated values are different from the rated values of the software model emulating a 2 MW wind turbine. The scaling of the voltage and current has to be performed to generate relevant outputs for the hardware and for the software. Table I gives the rated values for the two-level hardware converter and the model. The converter is designed to withstand an 90 A rms current and a 60 kW power, however, for proof-of-concept, the power and current are scaled down to 18kW and 25 A rms.

Table I: Wind farm model and hardware setup

Parameter	Wind farm model	hardware converter
Rated power	2 MW	18 kW
Rated voltage (L-L rms)	690 V	400 V
Rated current (rms)	1849 V	25 V

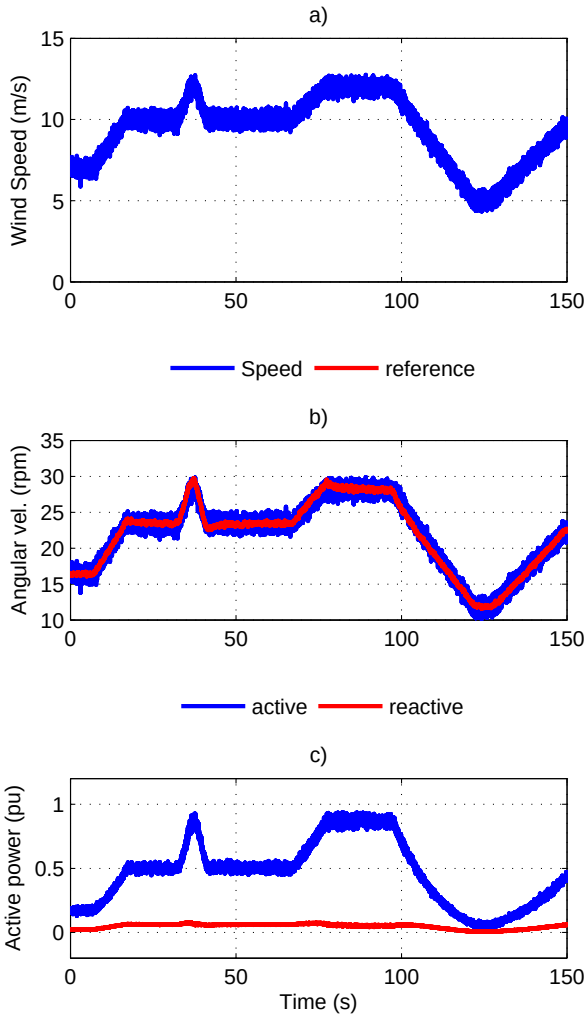

Figure 4: Real time emulation of the PMSG-based Wind turbine-Simulation

IV. Experimental Results

The simulated wind farm is designed assuming a 2 MW generation system connected to a 690 V and 50 Hz grid and operating at 1500 V in the dc side. The wind farm have been scaled down to 18 kW in order to interact with the size of the lab equipment. The HVDC was emulated using two-level VSC. One of them operates in island mode at 400 V and 50 Hz grid while is emulated using the grid emulator as shown in Figure 3 which keep a constant dc voltage at 700 V. dc cables have not been emulated for simplicity. Table II shows the corresponding wind farm parameters,

Figure 4 shows the experimental results of the PHIL implementation described above. Figure 4 a) shows the imposed wind profile. Figure 4 b) shows the generator angular speed and its reference in rpm. Figure 4 c) shows the active power and reactive power in the generator. The wind profile consists of an ascent ramp that carries the speed from 5 to 10 m/s in about 10 s. A second ramp start at 70 s and increases the speed until 12 m/s. A third ramp decreases the wind speed 7 m/s in 25 s. Finally, a ramp increases the wind speed up to 10 m/s. Two wind gust increase and decrease the wind speed at t =35 s and t =120 s as shown in Figure 4a). A white noise in injected in the wind profile. As the wind speed is increased, the generator speed and the generated electrical power are gradually increased following the maximum power point until almost the rated wind speed is achieved at 80 s. In the steady state, the theoretical values of the generator speed, which is 30 rpm, and generated electrical power is about 2 MW, as can be verified in the experimental results. Notice that the rated wind speed, 13 m/s, is not achieved and both the rated rotor speed and power is slightly lower than the rated values. Figure 4 c) shows the active and reactive powers imposed by the grid emulator to the real converter. This power is scaled down until 18 kW.

The results presented below are obtained with a steady wind condition of 12 m/s. First, Figure 5a) shows the voltage of one phase is displayed for the three measurement points in Figure 3. The simulated voltage, which is fed into the simulation model, and the real converter are resembled as was expected. Notice that the real converter voltage is lagging by 30 degrees behind the grid emulator voltage due to the delta-wye transformer. This phase shift had to be taken into account during the implementation of the PHIL. The corresponding currents are displayed in Figure 5 b). Due to the harmonics in its voltage input, the model produces a distorted current as a reference for the grid emulator. However, the grid emulator is able to track properly the current reference imposed by the model. The distortion in the current is also expected due the harmonics in the input voltage.

V. Conclusion

Power hardware-in-the-loop approach combine hardware devices with software simulation. The hardware part allows a high fidelity of the results whereas, the software simulation part allows an extensive study of different cases at a reasonable cost. PHIL is an emerging approach still limited by the cost of the hardware devices and the difficulties in the setting up of experiments. In this paper the proposed grid integration of wind farm using HVDC system was evaluated in a grid-connection experiment as a proof of concept. The proposed approach proves to be a useful tool for testing and evaluation of simulated wind farms scenarios with hardware setups. The proposed system has been validated through a demanding case study where the wind turbine model was controlled properly, the power extracted from the wind being amplified and the close-loop behavior of the PHIL setup was stable and predictable.

VI. Future work

The future work for this work will be focused on:

- The improvement of the wind power generation model e.g. the implementation of pitch angle control will allow

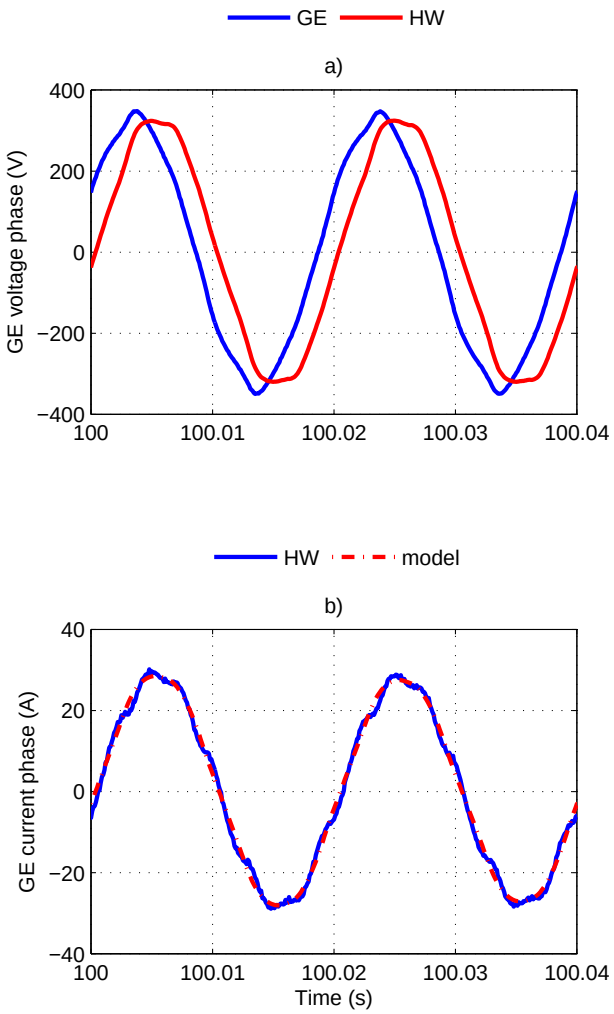

Figure 5: Real time emulation of the PMSG-based Wind turbine-Hardware

controlling the turbine without any restriction on the wind speed. A more realistic wind profile can improve the fidelity of the results.

- An aggregate model has been used. In the future, several wind turbines with different operating conditions can be connected to the hardware.
- The representation of the HVDC using two converters and new technologies such a modular multilevel concepts.

Acknowledgment

This project has received funding from the European Unions Seventh Programme for research, technological development and demonstration under grant agreement No 612748 (Best-Paths) and No. 609795 (IRP Wind). Authors would like to thank for the support.

VII. Appendix

Table II: Wind turbine parameters model

Parameters	Values	Units
Rated mechanical power	2.21	MW
Rated Voltage (line-to-line)	0.69	kV (rms)
Rated stator current	1849	A (rms)
Rated Stator Frequency	11.25	Hz
Rotor speed	30	rpm
d-axis synchronous inductance	1.21	mH
q-axis synchronous inductance	2.31	mH
Stator winding resistance	0.73	mΩ
Rated rotor flux linkage	14	V.s.
Number of pole pairs	30	
Total moment of inertia	100	kgm2
Rated Mechanical Torque	693	kNm

References

[1] O. Anaya-Lara, N. Jenkins, J. B. Ekanayake, P. Cartwright, and M. Hughes, *Wind energy generation: modelling and control*. John Wiley & Sons, 2011.

[2] L. Xu and B. Andersen, "Grid connection of large offshore wind farms using HVDC," *Wind Energy*, vol. 9, no. 4, pp. 371–382, 2006.

[3] P. Kundur, N. Balu, and M. Lauby, *Power system stability and control*, vol. 141. McGraw-Hill New York, 1994.

[4] P. Haugland, "Its time to connect: Technical description of HVDC light® technology," *Ludvika, Sweden: ABB Report*, 2006.

[5] R. Isermann, J. Schaffnit, and S. Sinsel, "Hardware-in-the-loop simulation for the design and testing of engine-control systems," *Control Engineering Practice*, vol. 7, no. 5, pp. 643–653, 1999.

[6] S. C. Oh, "Evaluation of motor characteristics for hybrid electric vehicles using the hardware-in-the-loop concept," *IEEE Transactions on Vehicular Technology*, vol. 54, no. 3, pp. 817–824, 2005.

[7] A. Martin and M. R. Emami, "An architecture for robotic hardware-in-the-loop simulation," in *Mechatronics and Automation, Proceedings of the 2006 IEEE International Conference on*, pp. 2162–2167, IEEE, 2006.

[8] A.-L. Allegre, A. Bouscayrol, J.-N. Verhille, P. Delarue, E. Chattot, and S. El-Fassi, "Reduced-scale-power hardware-in-the-loop simulation of an innovative subway," *IEEE transactions on Industrial electronics*, vol. 57, no. 4, pp. 1175–1185, 2010.

[9] L. Gauchia and J. Sanz, "A per-unit hardware-in-the-loop simulation of a fuel cell/battery hybrid energy system," *IEEE Transactions on Industrial Electronics*, vol. 57, no. 4, pp. 1186–1194, 2010.

[10] A. Bouscayrol, "Different types of hardware-in-the-loop simulation for electric drives," in *Industrial Electronics, 2008. ISIE 2008. IEEE International Symposium on*, pp. 2146–2151, IEEE, 2008.

[11] J. Wang, Y. Song, W. Li, J. Guo, and A. Monti, "Development of a universal platform for hardware in-the-loop testing of microgrids," *IEEE Transactions on Industrial Informatics*, vol. 10, no. 4, pp. 2154–2165, 2014.

[12] F. Huerta, R. L. Tello, and M. Prodanovic, "Real-time power-hardware-in-the-loop implementation of variable-speed wind turbines," *IEEE Transactions on Industrial Electronics*, vol. 64, no. 3, pp. 1893–1904, 2017.

[13] H. Li, M. Steurer, K. Shi, S. Woodruff, and D. Zhang, "Development of a unified design, test, and research platform for wind energy systems based on hardware-in-the-loop real-time simulation," *IEEE Transactions on Industrial Electronics*, vol. 53, no. 4, pp. 1144–1151, 2006.

[14] I. Munteanu, A. I. Bratcu, S. Bacha, D. Roye, and J. Guiraud, "Hardware-in-the-loop-based simulator for a class of variable-speed wind energy conversion systems: Design and performance assessment," *IEEE Transactions on Energy Conversion*, vol. 25, no. 2, pp. 564–576, 2010.

[15] A. Perdana, *Dynamic Models of Wind Turbines*. PhD thesis, Chalmers University of Technology, 2008.